

RSC Advances



This is an *Accepted Manuscript*, which has been through the Royal Society of Chemistry peer review process and has been accepted for publication.

Accepted Manuscripts are published online shortly after acceptance, before technical editing, formatting and proof reading. Using this free service, authors can make their results available to the community, in citable form, before we publish the edited article. This *Accepted Manuscript* will be replaced by the edited, formatted and paginated article as soon as this is available.

You can find more information about *Accepted Manuscripts* in the [Information for Authors](#).

Please note that technical editing may introduce minor changes to the text and/or graphics, which may alter content. The journal's standard [Terms & Conditions](#) and the [Ethical guidelines](#) still apply. In no event shall the Royal Society of Chemistry be held responsible for any errors or omissions in this *Accepted Manuscript* or any consequences arising from the use of any information it contains.

1 **Systemic research of Fluorescent Emulsion Systems and its**
2 **polymerization process with fluorescent probe by AIE mechanism**

3

4 Shengyuan Yang^a, Wenjun Shen^b, Weili Li^{†a,b,f*}, Jijun Tang^b, Wei Yao^b, Jun Wang^b, Mei
5 Fang Zhu^{a*}, Ben Zhong Tang^{c,d*}, Guodong Liang^e, Zexiao Xu^f

6 ^a State Key Laboratory for Modification of Chemical Fibers and Polymer Materials, Donghua
7 University, 2999 North Renmin Road 201620, China

8 ^b School of Material Science and Engineering, Jiangsu University of Science and Technology,
9 Zhenjiang 212003, China

10 ^c HKUST-Shenzhen Research Institute, No. 9 Yuexing 1st RD, South Area, Hi-tech Park, Nanshan,
11 Shenzhen 518057, China

12 ^d Department of Chemistry, Institute for Advanced Study, Institute of Molecular Functional Materials,
13 Division of Biomedical Engineering, Division of Life Science and State Key Laboratory of Molecular
14 Neuroscience, The Hong Kong University of Science & Technology (HKUST), Clear Water Bay,
15 Kowloon, Hong Kong.

16 ^e DSAP lab, PCFM lab, GDHPPC lab, School of Chemistry and Chemical Engineering, Sun Yat-Sen
17 University, Guangzhou 510275, China.

18 ^f Suzhou Jiren Hi-Tech Material Co., Ltd, Suzhou 215143.

19

20

21

22

23

24

25

26

27

28

29

30 **Abstract:** In this paper, AIE luminogen, which was used as a fluorescent probe, was
31 synthesized and copolymerized with acrylate monomers to study the process of
32 emulsion polymerization and the properties of fluorescent emulsion. At first,
33 according to the changes in fluorescence spectra, emulsion polymerization process can
34 be marked with real-time monitoring. Then, by varying the relative content of AIE
35 luminogen, glass transition temperature of the synthesized emulsion, the size of the
36 emulsion particle, the content of emulsion, and the detection temperature, etc. the
37 interaction between fluorescence properties and the intrinsic properties of the
38 emulsion were studied systematically. It should point out that the microscopic motion
39 of the segment of polymer can be studied by Fluorescence spectra with the help of
40 fluorescent probe. Traditionally, AIE luminogens are applied in optoelectronics and
41 biological domains at the state of small organic molecules. When AIE luminogen is
42 connected with polymer chains by chemical bond, a lot of interesting phenomenon
43 can be found. The research results not only provide a new method to study emulsion
44 polymerization process and the properties of emulsion, but also the synthesized
45 emulsion with the properties of fluorescence may broaden the application of AIE
46 mechanism.

47 **Key Words:** emulsion polymerization; fluorescent acrylate emulsion;
48 aggregation-induced emission; fluorescence spectrum; glass transition temperature

49 **Introduction**

50 Polymer particles have attracted a great deal of interest and have been utilized
51 in a wide range of fields^[1]. Waterborne polymer colloids, often referred to as
52 ‘emulsion dispersions’, are well-established for diverse applications in many
53 commercial products from different industrial segments including cosmetics,
54 pharmaceuticals, adhesives, coatings and paints^[2-5]. A key advantage of the colloidal
55 approach is that it enables direct control of internal structure organization of the
56 particles at nanoscale^[6]. Nanostructured lattices have been commonly prepared by
57 emulsion polymerization processes in the presence of emulsifying agents to ensure the
58 physical stability and the nanometric size of the resultant particles. Examples of

59 miniemulsion, suspension or dispersion polymerization processes can be found in the
60 literature but emulsion polymerization is by far the most frequently used technique ^[7].
61 TraditionAE methods to study emulsion and emulsion polymerization process
62 including FTIR, ¹H NMR or ¹³C NMR, DSC, TGA, TEM, SEM, and Laser
63 Diffraction Particle Size Analyzer to study their chemical substance, their structure,
64 morphologies, and thermodynamic performance^[1,7]. However, as the multiphase
65 system, a lot of research conclusion about it is still obscure, and it still need to carry
66 on further investigation to research the properties of emulsion and systematically.

67 Beside studying the intrinsic properties of the emulsion, the functionalization of
68 emulsion particles is also the important research work. When fluorescent molecule
69 were incorporated into the emulsion particles, they attracted increasing interest owing
70 to their potential applications ranging from optoelectronics to biological imaging and
71 disease therapy^[8]. Incorporation of polymerizable organic dyes including uoresceins,
72 rhodamines, 1,8-naphthalimides, diverse aromatic dyes, coumarins, azo-dyes and
73 oxadiazoles into polymers using polymerization methods including free radical
74 polymerization, reversible addition-fragmentation transfer polymerization, atom
75 transfer radical polymerization, nitroxide mediated polymerization and emulsion
76 polymerization etc. have been reported^[8]. However, these fluorescent organic particle
77 based on conventional organic dyes often lead to a significant decrease of their
78 fluorescent intensity after their self-assembly into nanoparticles because of the
79 notorious aggregation-caused quenching effect^[9,10].

80 In 2001, a novel phenomenon of aggregation-induced emission(AIE) was first
81 found by Tang's group from propeller-like siloles, whose emission was very weak in
82 solution but became intense as aggregates formed^[11]. Such abnormal emission
83 behavior has drawn great research interest, for it is exactly opposite to the common
84 belief that the emission of chromophores decreases in the aggregate state^[12-14]. This
85 intriguing finding paves a new avenue to tackle the notorious ACQ of conventional
86 chromophores. Bin Liu and Ben zhong Tang *et al* synthesized TPE-TPA-DCM,
87 fabricated its BSA nanoparticles, and explored their in vivo and in vitro bioimaging

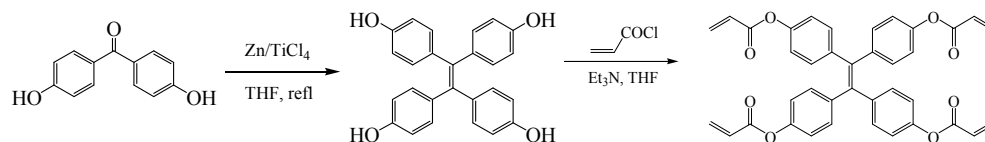
88 applications. The TPE-TPA-DCM possesses both TICT and AIE features, and its
89 BSA-formulated NPs show efficient FR/NIR fluorescence with low cytotoxicity,
90 uniform size and spherical morphology^[15]. Xiaoyong Zhang, Yen Wei *et al* obtained
91 polymer nanoparticles (named as PhE–Pst NPs) exhibited strong fluorescence and
92 high water dispersibility owing to the partial aggregation of PhE and the surface
93 covered with a hydrophilic shell. More importantly, these FONs showed spherical
94 morphology, uniform size (about 200 nm) and excellent biocompatibility, making
95 them promising for bioimaging applications^[16]. Tang *et al* reported highly emissive
96 AIE-based inorganic-organic nanoparticles with core–shell structures which were
97 fabricated by a one-pot, surfactant-free hybridization process. The resultant FSNPs
98 were mono dispersed with smooth surfaces. They possessed high surface charges,
99 AIE features and excellent colloidal stability. Furthermore, the particle diameters and
100 emission efficiencies of the FNPs could be manipuiable by changing the reaction
101 conditions and luminogen loadings^[17,18].

102 Although fluorescent organic particles had been studied for a long time and
103 showed great prospects in application, the relationship between their fluorescent
104 property and other intrinsic properties still need to be researched carefully. In this
105 paper, tetraphenylethene-containing tetra-acrylates was synthesized and used as a
106 fluorescent probe to carry on the systematic research work. Tetraphenylethene (TPE),
107 as one of the typical fluorescent molecule with AIE character, is found to be
108 non-emissive in dilute solutions but became highly luminescent when their molecules
109 are aggregated in concentrated solutions or cast in solid films^[19]. In detail, in a dilute
110 solution, TPE undergoes dynamic intramolecular rotations against its double bound
111 and renders its molecule non-luminescent. On the other hand, in the aggregate state,
112 the molecules cannot pack through a π - π stacking process due to its propeller shape,
113 while the intramolecular rotations of its aryl rotors are greatly restricted owing to the
114 physical constraint. This restriction blocks the non-radiative pathway and opens up
115 the radiative channel^[20-21]. Taking the advantage of its unique properties, the
116 fluorescence intensity of the polymer modified with TPE-containing tetra-acrylate can

117 be efficiently enhanced by increasing its concentration, loading without the need to
118 avoid the aggregation of the probes. It is possible to study the emulsion
119 polymerization process and the properties of emulsion through fluorescence spectrum
120 by taking advantage of AIE mechanism.

121 Results and discussion

122 Tetraphenylethene-containing tetra-acrylates was synthesized according to the
123 previous document^[22]. Briefly, McMurry coupling reaction of
124 4,4'-dihydroxybenzophenone catalyzed by TiCl_4 -Zn in THF generated intermediate
125 tetrahydroxy tetraphenylethene. Since it readily underwent oxidation reaction in air,
126 they were treated with acryloyl once isolated to furnish the product, TPE-containing
127 tetra-acrylate. White solid; overall yield 38%. Detail structural analyses are provided
128 in the Fig. 1S.



129

130

Scheme 1 Synthesis of TPE-containing tetra-acrylate

131 The standard emulsion polymerization process was carried on as follows. The
132 synthesized TPE-containing tetra-acrylate was blended with acrylate monomers and
133 prepared fluorescent acrylate emulsion *via* emulsion polymerization with sodium
134 dodecyl sulfate (SDS) as the emulsifying agent and potassium persulfate (KPS) as the
135 thermal initiator. In brief, acrylate monomers mixed with AIE luminogen were
136 dispersed in water, which contained a minute amount of the emulsifying agent and
137 thermal initiator. After the blending mixtures were emulsified with intense mixing, the
138 polymerization was carried out at 80°C for 10h with continuous stirring. Different
139 conditions were set to study the interaction between fluorescence properties and the
140 other intrinsic properties of the emulsion, such as the relative content of AIE
141 luminogen, the size and the content of fluorescent acrylate emulsion, the glass
142 transition temperature of the polymers, and the detection temperature. To identify the
143 samples accurately, the prepared different fluorescent acrylate emulsions are named
144 from AE-TPE-A to AE-TPE-R. Detailed contents of the preparation process are

145 presented in the supporting materials.

146 At first, sample AE-TPE-D was selected as the example to study emulsion
147 polymerization process, which is presented in Fig.1. During the process of
148 polymerization, AIE luminogen acted as the probe to tracking the whole reaction
149 process according to fluorescence spectrum. Owing to the electronic transition of the
150 TPE unit, the absorption spectra of TPE-containing tetra-acrylate and fluorescent
151 acrylate emulsion exhibited the absorption peak at around 460nm.

152 ----- **Fig.1** -----

153 **Fig.1(a)** Fluorescence spectra of ongoing reacting fluorescent acrylate emulsion; (b) Wavelength
154 and intensity of PL spectra of ongoing reacting fluorescent acrylate emulsion and (c) Pictures of
155 ongoing reacting fluorescent acrylate emulsion taken by camera varied with reaction time (From 5
156 to 600min)

157 At first, no obvious polymerization phenomenon happened before 50min
158 according to the pictures taken from camera and the results of fluorescence spectra.
159 During this stage, AIE luminogen was just physical dispersed into micelles with
160 methylmethacrylate monomer, and thermal initiators started to decompose and
161 generate free radicals in water. The fluorescence spectra of AIE luminogen showed a
162 distinct emission peak at around 485nm because of the poor solvent system. However,
163 with the reaction carrying on, autoacceleration effect^[23] happened from 55min due to
164 higher concentration of monomers and free radicals in the micelles. The peak position
165 red shifted to 455nm and the intensity enhanced for about fourteen times. We have
166 proposed that restriction of intramolecular rotation (RIR) is the main cause for the
167 AIE phenomenon^[24]. When AIE luminogen and monomers are knitted together by
168 covalent bonds to form polymer chains, the RIR process will partially activate. This
169 restriction blocks the non-radiative pathway and opens up the radiative channel^[25],
170 and thus make the synthesized acrylate emulsion somewhat emissive. From 55min to
171 120min, in the second process of polymerization, more intramolecular rotation of AIE
172 luminogen was restricted due to more of it had reacted and formed the polymer chains.
173 According to AIE mechanism, the fluorescence intensity increased with the content of
174 the reacted AIE luminogens. So in this stage, fluorescence intensity of the reacting

175 system increased with the time. With the reaction continued, the fluorescence intensity
176 of the reaction system maintained a relatively stable state from 120min to 300min. It
177 meant that AIE luminogens had been ran out of during the third stage. However, due
178 to metastable nature of acrylate emulsion, it might collide, aggregate and deposit at
179 high temperature. So, with the reaction preceded, a part of fluorescent acrylate
180 emulsion formed gel and precipitated, and the fluorescence intensity decreased with
181 reacting time.

182 To verify the results of fluorescence spectra, GPC and solid content of the
183 emulsion measurements were carried on. As can be seen from the supporting
184 materials, the results of them confirm the result fluorescence spectra. Typical process
185 of emulsion polymerization can be summarized as follows: In the beginning, the
186 reactive monomers were wrapped in the micelles formed by emulsifying agent and
187 dispersed in water. At this stage, the content of the free radicals was quite low, and the
188 reaction proceeded gently. With the reaction carried on, the concentration of free
189 radicals increased gradually, and part of them entered into the micelles. Because the
190 concentration of reaction monomers in the micelles is quite high, auto-acceleration
191 effect of free-radical polymerization happened during this stage, and most of
192 monomers (over 90%) reacted. The residual monomers consumed gradually in the
193 next two or three hours. Due to acrylate emulsion was a metastable system, some of
194 emulsion particles might collide, aggregate and deposit in the last stage.

195 Fig.2(a) presents the fluorescent acrylate emulsion (AE-TPE-D) and
196 commercial purchased acrylate emulsion under UV light (365nm). Owing to the AIE
197 mechanism as mentioned above, the synthesized AE-TPE-D emitted a strong
198 fluorescence. Fig.2(b) represents the typical morphology of the synthesized
199 fluorescent acrylate emulsion (AE-TPE-D) from TEM measurement. With the packing
200 of micelle formed by emulsifying agent, acrylate monomers and AIE luminogens
201 were dispersed and polymerized in the micelles *via* emulsion polymerization^[26]. The
202 fluorescent acrylate emulsion presented typical core-shell structure, in which
203 hydrophobic properties of methylmethacrylate and AIE luminogens were wrapped
204 into the core layer of the fluorescent acrylate emulsion, while the emulsifying agent

205 with amphipathic property formed the shell layer to make them be dispersed in water.
206 With these characteristics, the composition of the fluorescent acrylate emulsion, the
207 preparation process and the external environment can influence the fluorescence
208 property of the synthesized fluorescent acrylate emulsion. So in the next, we will
209 study the interrelationships between them systematically.

210 ----- **Fig.2** -----

211 **Fig.2** (a) Fluorescent acrylate emulsion and ordinary acrylate emulsion irradiated under UV light

212 (b) Fluorescent acrylate emulsion observed from TEM measurement

213 At first, take AE-TPE-D and TPE-containing tetra-acrylate as examples, the
214 interaction between AIE luminogen and polymer chains was studied, and their
215 fluorescence spectra were presented in Fig.3. As we know the result of fluorescence
216 spectroscopy was the relative value, the contents of AIE luminogens of two samples
217 were identical to study their fluorescence properties. Compared to pure
218 TPE-containing tetra-acrylate in THF-water (1:99) mixture, the emission peak of
219 AE-TPE-D is at about 455nm, which blue shifted about 30 nm. Also, it should point
220 out that the fluorescent intensity increases by about 7 times for AE-TPE-D at the
221 content of AIE luminogen. It should partly attribute to the wrapping and coiling of
222 rigid polymer chains^[27]. As to small AIE luminogen, it tends to aggregate in its poor
223 solvent and radiate fluorescent light when it is induced by UV light, however, their
224 aggregation is activated just by physical stacking. When it is knitted to rigid polymer
225 chains with chemical bond, its intramolecular rotation may be restricted even harder.
226 So higher absorbed energy can be released by fluorescent light, the emission peak
227 tends to blue shift, and the fluorescent intensity also increases.

228 ----- **Fig.3** -----

229 **Fig.3** Fluorescence spectra of TPE-containing tetra-acrylate in THF-water (1:99) mixture and

230 Fluorescent Acrylate emulsion (AE-TPE-D)

231 The fluorescent property of fluorescent acrylate emulsion which is affected by
232 the relative content of AIE luminogen is presented in Fig.4. It is obviously that the
233 peak intensity increased linearly with the content of TPE-containing tetra-acrylate for
234 the sample from AE-TPE-A to AE-TPE-D. This is inaccessible to ACQ probes such as

235 pyrene, where increasing the concentration of probes leads to the formation of
236 excimers or aggregates and consequent fluorescence quenching^[28-30]. For AIE
237 luminogens such as TPE-containing tetra-acrylate, aggregation favors emission, and
238 thus allows the enhancing of fluorescence intensity by increasing AIE luminogen
239 loading^[31]. However, for the sample AE-TPE-E, its fluorescence intensity decreases
240 when compared to AE-TPE-D. With four functional groups of AIE luminogen, the
241 stability of the synthesized fluorescent acrylate emulsion may be affected by it due to
242 cross linking polymerization. When the content of AIE luminogen extends to a certain
243 limit, some of the synthesized fluorescent acrylate emulsion tends to gather and
244 precipitate due to excessive cross-linking. So it is understandable that the peak
245 intensity of AE-TPE-E is lower than AE-TPE-D because some of AIE luminogens
246 have been precipitated. To confirm this conclusion, we also measured the
247 fluorescence quantum yield(Φ_F) of fluorescent acrylate emulsions varied with the
248 content of AIE luminogen and the results are summarized in Fig.5 and Table 1,
249 respectively. The trend of Φ_F of different fluorescent acrylate emulsions also indicate
250 that the content of AIE luminogens will determine the luminescence behavior of the
251 fluorescent acrylate emulsions, and it increases with the content of AIE luminogen
252 according to AIE mechanism.

253 ----- **Fig.4** -----

254 **Fig.4** Fluorescence spectra of fluorescent acrylate emulsion varied with the content of
255 TPE-containing tetra-acrylate

256 ----- **Fig.5** -----

257 **Fig.5** Fluorescence quantum yield(Φ_F) of fluorescent acrylate emulsions varied with the
258 content of AIE luminogen

259 ----- **Table 1** -----

260 **Table 1** Optical properties of fluorescent acrylate emulsion varied with the content of
261 TPE-containing tetra-acrylate

262 Fluorescent acrylate emulsions of different sizes varied with the content of
263 emulsifying agent were prepared and studied. Fig.4S presents their particle size and
264 particle size distribution. From Fig.6, the fluorescent intensities increase with the

265 decreased size of fluorescent acrylate emulsion particles. As is presented in Fig.2(b),
266 the fluorescent acrylate emulsion particles present a typical core-shell structure and
267 AIE luminogens with hydrophobic property are wrapped in the inner core. With the
268 size of fluorescent acrylate emulsion decreasing, the space for segmental motion of
269 polymer chains in the fluorescent acrylate emulsion particles becomes smaller. The
270 restricted movement of polymer chains will strengthen RIR effect of AIE luminogens
271 because it is knitted to rigid polymer chains with chemical bond.

272 ----- **Fig.6** -----

273 **Fig.6** Fluorescence spectra of fluorescent acrylate emulsion varied with particle size

274 Sample AE-TPE-D was selected to study the relationship between fluorescent
275 property and the content of fluorescent acrylate emulsion by the addition of water
276 (Fig.7). From Sample AE-TPE-D to Sample R, the fluorescent intensities of the
277 samples increase with the decreased concentration. For the synthesized fluorescent
278 acrylate emulsion, its component and particle size were fixed. According to AIE
279 mechanism, their fluorescent intensity should decrease with the concentration of AIE
280 luminogens. However, contrary to theoretical analysis, its fluorescent intensity
281 increased in fact. We deem that the changed polarity and the squeezing effect of
282 hydrophilic layer may be the reasons for this phenomenon. As the AIE luminogens are
283 knitted to the polymer chains by chemical bonds, their fluorescence properties will be
284 affected by polymer segmental motion. The polarity of system was increased with the
285 added water, which will block the segment motion of hydrophobic polymer chains^[32].
286 In addition, the increased squeeze force of the hydrophilic layer by the added water
287 may enhance this effect. All of these influences can reinforce the RIR effect of AIE
288 luminogens.

289 ----- **Fig.7** -----

290 **Fig.7** Fluorescence spectra of fluorescent acrylate emulsion(AE-TPE-D) varied with their
291 concentration

292 Testing temperature was set to be at 25°C, different acrylate emulsions varied
293 with T_g value were studied by fluorescence spectra. From Fig.8(a), by increasing glass
294 transition temperature, the fluorescence intensity increases. In addition, the peak

295 positions can be changed also. The peak positions of fluorescent acrylate emulsions
296 were at around 455nm when their T_g values were higher than room temperature, while
297 for those fluorescent acrylate emulsions whose T_g were lower than room temperature,
298 their peak positions were at around 470nm. A possible reason is that in the glassy state,
299 the intramolecular motions of phenyl rings of AIE luminogens are restricted to some
300 extent when they are knitted and embedded in the rigid polymer matrices. The energy
301 of the excited state is annihilated through radiation decay, and thus the fluorescent
302 acrylate emulsions emits efficiently. When the polymers are in the rubbery state,
303 intramolecular motions of AIE luminogens are activated due to the movement of
304 polymer segments and significantly increased free volume in the polymer matrices.
305 The intramolecular motions consume the energy of the excited state. This leads to the
306 weak and red shift of fluorescence emission in the rubbery state of the polymers^[11,33].

307 ----- **Fig.8** -----

308 **Fig.8(a)** Fluorescence spectra of fluorescent acrylate emulsions varied with their T_g values, (b)
309 Fluorescent wavelength & intensity of fluorescent acrylate emulsion varied with their T_g values

310 SEM images of the coatings cured at room temperature for different fluorescent
311 acrylate emulsions varied with T_g values are presented in Fig.5S. As we know, the
312 process of film formation for ordinary emulsion is carried on as follows: at first, the
313 emulsion particles are aggregated by the evaporation of water; then they tend to be
314 warped and destroyed due to the capillary forces between the gap of emulsion
315 particles; finally, the damaged emulsion particles tend to intermix with each other and
316 form a flat coating on the substrate surface. T_g value of emulsion can determine the
317 film forming ability of the emulsion particles. For those emulsion particles whose T_g
318 value lower than room temperature, soft polymer chains benefit to the deformation of
319 emulsion particles and form a flat coating. While for those emulsions with high T_g
320 value (beyond room temperature, 25°C), the emulsion particles cannot wrap due to
321 stiff polymer chains, and they still present as a nano-sized particles after the
322 evaporation of water. According to AIE mechanism, trace amount of AIE luminogen
323 can be used as the fluorescent probe to study the film forming ability of the emulsion
324 particles.

325 Glass transition is the intrinsic property of amorphous polymers, and it is the
326 macro-reflection of the transformation for the movement of polymer chains, which
327 will affect the materials' use properties and processability^[34,35]. According to
328 Molecular Structural Theory, glass transition is the relaxation phenomenon for the
329 amorphous area of polymer materials from freeze state to unfrozen state. At the room
330 temperature under T_g , only atom or functional groups on the polymer chains can
331 vibrate at the equilibrium position. In addition, according to the mechanical properties
332 of the polymer materials, the whole glass transformation region of polymers materials
333 can be divided into "tough" glass state and "soft" glass state. The temperature to
334 identify these two states was brittle temperature (T_b)^[36]. For the temperature is lower
335 than T_b , the polymer materials present brittleness property; however, when the
336 temperature is higher than T_b , the polymer materials present extensibility.

337 As is presented in Fig.9, AE-TPE-P, whose T_g is set as 40°C, is used as the
338 example to study the interrelation between fluorescent property of fluorescent acrylate
339 emulsions and the test temperature. As the segmental motion ability increases with the
340 increased temperature, according to RIR mechanism, intramolecular motions of TPE
341 are activated due to the movement of polymer segments and significantly increased
342 free volume in the polymer matrices. So the fluorescence intensity decreases with the
343 increased test temperature. It should be pointed out that there are two apparent
344 lowering platforms for the decreased PL intensity in the glass transition region. As is
345 discussed above, there are "tough" glass state and "soft" glass state of the amorphous
346 polymers. Although the subtle changes varied with temperature of the polymer chains
347 cannot be observed from ordinary DSC measurement (Fig.10(a)), however, it might
348 be informed indirectly from fluorescent spectra because the fluorescent probe and
349 polymer chains was knitted together at molecular level with covalent bond, polymer
350 segmental motion can affect the fluorescent luminescence behavior of the fluorescent
351 acrylate emulsions directly. From Fig.10(b), fluorescent intensity of the dried
352 AE-TPE-P varied with test temperature were presented. For polymer matrix, its
353 segmental motion at solid state could not pretty obvious compared to it is dispersed in
354 the emulsion particles due to high packing density of polymer chains at solid state.

355 From the trend of fluorescence intensity varied with temperature, T_g value of the
356 synthesized emulsion can be obtained, which closes to the theoretical calculation
357 value.

358 ----- **Fig.9** -----

359 **Fig.9** (a) Fluorescence spectra of fluorescent acrylate emulsion (AE-TPE-P, $T_g=40^\circ\text{C}$) varied with
360 the testing temperature, (b) fluorescent intensity of AE-TPE-P varied with the testing temperature

361 ----- **Fig.10** -----

362 **Fig.10** Study the properties of the dried AE-TPE-P powers by different testing methods (a) DSC
363 thermograms; (b) Fluorescence spectra

364 **Conclusion**

365 Due to AIE luminogen tetraphenylethene-containing tetra-acrylates is knitted
366 with polymer chains by chemical bond, and the synthesized fluorescent emulsion
367 particles are dispersed in water uniformly, the changes of the emulsion system and the
368 segmental motion of polymer matrix will affect the fluorescent properties of AIE
369 luminogen owing to the restriction of intramolecular rotation (RIR) effect. With this
370 characteristic, the process of emulsion polymerization can be monitored on real-time,
371 and the changes with its internal characteristics and external environments can
372 interfere fluorescence spectrometry of the emulsion directly. This study thus opens up
373 a new avenue for the research of the emulsion polymerization process and develops
374 AIE-active emulsion. In addition, the synthesized emulsion with the properties of
375 fluorescence may broaden the application of AIE mechanism.

376 **Materials**

377 THF was distilled under normal pressure from sodium benzophenone ketyl under
378 nitrogen immediately prior to use. 4,4'-dihydroxybenzophenone, zinc powder,
379 titanium(IV) chloride(TiCl_4), triethylamine, acryloyl chloride, methylmethacrylate
380 (MMA,C.P.), ethylhexyl acrylate(2-EHA,C.P.), dodecyl sulfate(SDS, A.R.), and
381 potassium persulfate(KPS, A.R.) were used as received without further purification.

382 **Instruments**

383 ^1H NMR spectra were measured on Bruker ARX 400 NMR spectrometers using

384 CDCl_3 as the deuterated solvent and tetramethylsilane (TMS; $\delta=0\text{ppm}$) as the internal
385 standard. FTIR spectra were recorded on a Perkin-Elmer 16 PC FT-IR
386 spectrophotometer. Relative number (M_n) and weight-average (M_w) molecular
387 weights and polydispersity indices (PDI or M_w/M_n) of the fluorescent emulsion
388 particles were estimated by a Waters Associates Gel Permeation Chromatography
389 (GPC) system equipped with RI and UV detectors. THF was used as the eluent at a
390 flow rate of 1.0 mL min^{-1} . A set of monodispersed linear polystyrenes covering the
391 molecular weight range of $10^3\sim 10^7$ were used as the standard for the molecular weight
392 calibration. DSC measurements were carried out using DSC Q100 (TA Instruments)
393 (TA Instruments, USA) over the temperature of -50°C to 150°C at a scan rate of 10°C
394 min^{-1} . The thermogram was base line corrected and calibrated using Indium metal.
395 The experimental specimens (8–10 mg) were dried at 60°C under vacuum for 24h,
396 before being measured. All the samples were firstly annealed at 120°C for 3 min, and
397 cooled to -50°C by using liquid nitrogen and then scanned for the measurement.
398 UV-vis absorption and light transmission spectra were measured on a Milton Roy
399 Spectronic 3000 array spectrophotometer. Fluorescence spectra were recorded using a
400 steady state spectrometer (Edinburgh Instrument Ltd, FLSP920) equipped with a
401 temperature control system (Oxford instruments). To eliminate the interference of
402 heating rates on the thermal properties of the fluorescent elastomer, heating rate was
403 fixed at 1 min^{-1} for all specimens. Fluorescence spectra were scanned every 1 min.
404 The absolute Fluorescence quantum yield(Φ_F) of fluorescent acrylate emulsions
405 was measured using an integrating sphere (FLS 980, Edinburgh). Images of scanning
406 electron microscopy(SEM) was taken on a JSM-6700F electron microscope. Image of
407 and transmission electron microscope(TEM) was taken on
408 JEOL 2010 transmission electron microscope (TEM) at accelerating voltages of 200K
409 V . Particle sizes of the fluorescent emulsion particles were measured on a
410 Brookhaven Instruments Corporation 90 Plus/B1-MAS Zetaplus Zeta Potential
411 Analyzer.

412 Acknowledgements

413 The project was funded by State Key Laboratory for Modification of Chemical
414 Fibers and Polymer Materials, Donghua University, NSFC (No.21201087), and
415 Postdoctoral Foundation of Jiangsu Province (NO.1501091c). Author also thanks
416 Jiangsu Overseas Research & Training Program for University Prominent Young &
417 Middle-aged Teacher and Presidents, and the Innovative Programs for Undergraduate
418 Students of and Innovative Programs for Graduate Students of Jiangsu University of
419 Science and Technology. We thank Dr Hongkun Li from Soochow University to help
420 us to carry on the fluorescence quantum yield measurement.

421 References

- 422 1. A. M. Aerds, A. M. van Herk, B. Klumperman, J. Kurja, A. L. German, *Synthesis of Polymers*,
423 2008, 268-316.
- 424 2. T. Wang, J.L. Keddie, *Adv. Colloid. Interface Sci.*, 2009, **147-148**, 319-332.
- 425 3. J.M. Asua, *Prog. Polym. Sci.*, 2014, **39**, 1797-1826.
- 426 4. A.P. Richez, H.N. Yow, S. Biggs, O.J. Cayre, *Prog. Polym. Sci.*, 2013, **38**, 897-931.
- 427 5. K. Shen, Y. Wang, G. Ying, M. Liang, Y. Li, *Colloids Surf. A*, 2015, **467**, 216-223.
- 428 6. A.M. Oliveira, K.L. Guimarães, N.N.P. Cerize, *European Polymer Journal*, 2015, **71**, 268-278.
- 429 7. T. F. Tadros, *Emulsion Formation, Stability, and Rheology*, 2013, 1-75.
- 430 8. A. M. Breul, M. D. Hager and U. S. Schubert, *Chem. Soc. Rev.*, 2013, **42**, 5366-5407.
- 431 9. C.H. Ren, H.M. Wang, D. Mao, X.L. Zhang, Q.Q Fengzhao, Y. Shi, D. Ding, D.L. Kong, L. Wang
432 and Z.M. Yang, *Angew. Chem.-Int. Edit.*, 2015, **54(16)**, 4823-4827.
- 433 10. Y.Y. Yuan, R. T. K. Kwok, B. Z. Tang and B. Liu., *Small*, 2015, **11(36)**, 4682-4690.
- 434 11. J. Luo, Z. Xie, J. W. Y. Lam, L. Cheng, B. Z. Tang, H. Chen, C. Qiu, H. S.Kwok, X. Zhan, Y. Liu
435 and D. Zhu, *Chem. Commun.*, 2001, 1740-1741.
- 436 12. Y. N. Hong, J. W. Y. Lam and B. Z. Tang, *Chem. Commun.*, 2009, 4332-4353.
- 437 13. J. Mei, Y. N. Hong, J. W. Y. Lam, A. J. Qin, Y. H. Tang and B. Z. Tang, *Adv. Mater.*, 2014, **26**,
438 5429-5479.
- 439 14. R. R. Hu, N. L. C. Leung and B. Z. Tang, *Chem. Soc. Rev.*, 2014, **43**, 4494-4562.
- 440 15. W. Qin, D. Ding, J. Z. Liu, W. Z. Yuan, Y. Hu, B. Liu, and B. Z. Tang, *Adv. Funct. Mater.*, 2012,
441 **22**, 771-779.

- 442 16. X.Y. Zhang, X.Q. Zhang, B. Yang, M.Y. Liu, W.Y. Liu, Y.W. Chen and Y. Wei, *Polym. Chem.*, 2014,
443 5, 399–404.
- 444 17. F. Mahtab, Y. Yu, J. W. Y. Lam, J. Z. Liu, B. Zhang, P. Lu, X. X. Zhang and B. Z. Tang, *Adv.*
445 *Funct. Mater.*, 2011, **21**,1733–1740.
- 446 18. M. Li, J. W. Y. Lam, F. Mahtab, S.J. Chen, W.J. Zhang, Y.N. Hong, J. Xiong, Q.C. Zheng, and B.
447 Z. Tang, *J. Mater. Chem. B*, 2013, **1**, 676–684.
- 448 19. Z. F. Chang, Y. B. Jiang, B. R. He, J. Chen, Z. Y. Yang, P. Lu, H. S. Kwok, Z. J. Zhao, H. Y. Qiu
449 and B. Z. Tang, *Chem. Commun.*, 2013, **49**, 594-596.
- 450 20. J. Yang, N. Sun, J. Huang, Q.Q. Li, Q. Peng, X. Tang, Y.Q. Dong, D.G. Ma and Z. Li, *J. Mater.*
451 *Chem. C.*, 2015, **3**, 2624-2631.
- 452 21. J. Q. Shi, N. Chang, C. H. Li, J. Mei, C. M. Deng, X. L. Luo, Z. P. Liu, Z. S. Bo, Y. Q. Dong and B.
453 Z. Tang, *Chem. Commun.*, 2012, **48**, 10675-10677.
- 454 22. R. R. Hu, J. W. Y. Lam, Y. Yu, Herman H. Y. Sung, Ian D. Williams, Matthew M. F. Yuen and B. Z.
455 Tang, *Polym. Chem.*, 2013, **4**, 95-105.
- 456 23. E. Mastan, X.H. Li, and S.P. Zhu, *Prog. Polym. Sci.*, 2015, **45**, 71-101.
- 457 24. Q. S. Liu, X. Q. Wang, H. Yan, Y. P. Wu, Z. Y. Li, S. W. Gong, P. Liu and Z. P. Liu, *J. Mater. Chem.*
458 *C*, 2015, **3**, 2953-2959.
- 459 25. W.L. Li, D. Huang, J. Wang, W.J. Shen, L.Z. Chen, S.Y. Yang, M.F. Zhu, B. Z. Tang, G. D. Liang
460 and Z.X. Xu, *Polyme. Chem.*, 2015, **6**, 8194–8202.
- 461 26. S. Krishnan, A. Klein, M. S. El-Aasser, and E. DavidSudol, *Macromolecules*, 2003, **36 (9)**, 3152–
462 3159.
- 463 27. A. Pucci, G. Iasilli, F. Tantussi, F. Fuso and G. Ruggeri, *6th International Conference on Times of*
464 *Polymers(TOP) and Composites AIP Conf. Proc.*, 2012, **1459**, 89-91.
- 465 28. S. Farhangi, H. Weiss and J. Duhamel, *Macromolecules*, 2013, **46**, 9738–9747.
- 466 29. S. H. Chen, J. Duhamel and M. A. Winnik, *J. Phys. Chem. B*, 2011, **115**, 3289–3302.
- 467 30. Y. Rharbi, L. S. Chen and M. A. Winnik, *J. Am. Chem. Soc.*, 2004, **126**, 6025–6034.
- 468 31. G. D. Liang, Jacky W. Y. Lam, W. Qin, J. Li, N. Xie and B. Z. Tang, *Chem. Commun.*, 2014, **50**,
469 1725-1727.
- 470 32. J.L Hu, Y. Zhu, H.H. Huang, J. Lu, *Prog. Polym. Sci.*, 2012,**37(12)**, 1720-1763.
- 471 33. J. D. Luo, Z. L. Xie, J. W. Y. Lam, L. Cheng, H. Y. Chen, C. F. Qiu, H. S. Kwok, X. W. Zhan, Y. Q.
472 Liu, D. B. Zhu and B. Z. Tang, *Chem. Commun.*, 2001, 1740–1741.

- 473 34. J. W. Chen, C. C. W. Law, J. W. Y. Lam, Y. P. Dong, S. M. F. Lo, I. D. Williams, D. B. Zhu and B.
474 Z. Tang, *Chem. Mater.*, 2003, **15**, 1535–1546.
- 475 35. Y.J Xing, Y.H. Wu, Y.Q. Zhou, G. Yang, W.L. Li, and L. X. Xu, *Electrochimica Acta* 2014, **136**,
476 513-520.
- 477 36. W.L Li, Y.H. Wu, J.W. Wang, D. Huang, L.Z. Chen, and G. Yang, *European Polymer Journal*,
478 2015,**67**,365-372.
- 479 37. H.-Y. Hsueh, C.T. Yao and R.-M. Ho, *Chem. Soc. Rev.*, 2015,**44**, 1974-2018 .
480

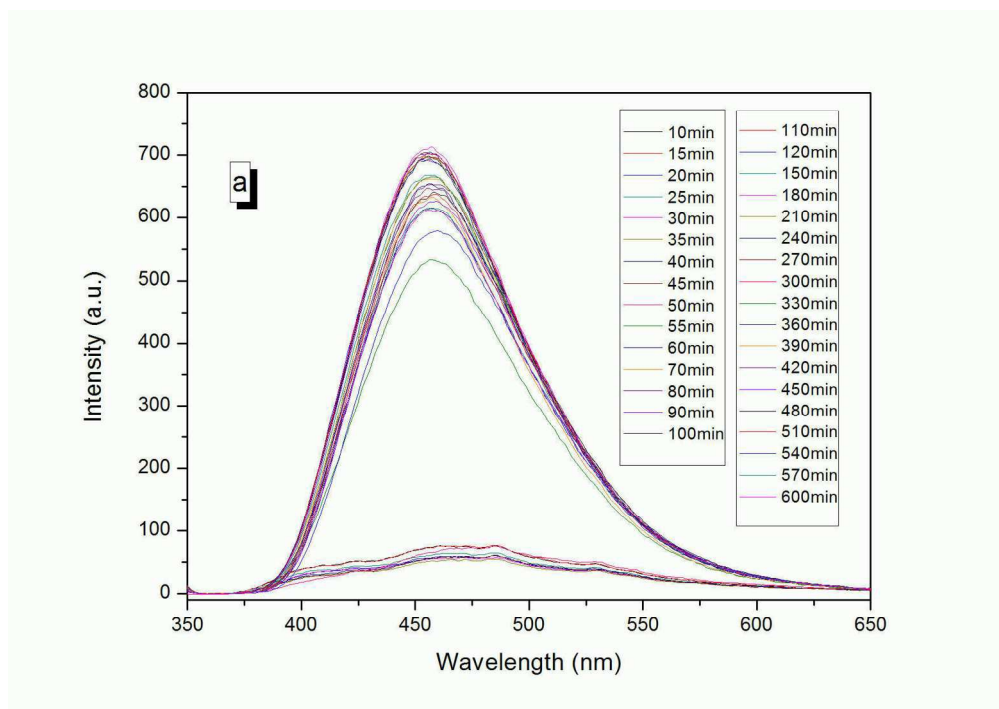


Fig.1(a) Fluorescence spectra of ongoing reacting fluorescent acrylate emulsion

464x328mm (96 x 96 DPI)

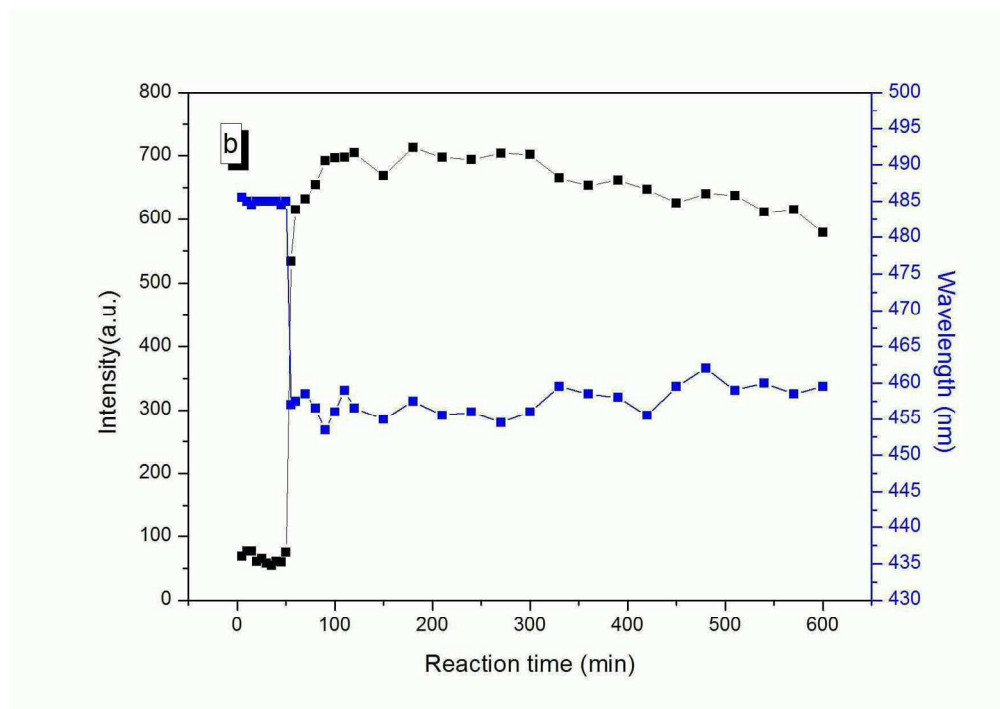


Fig.1(b) Wavelength and intensity of PL spectra of ongoing reacting fluorescent acrylate emulsion

464x328mm (96 x 96 DPI)

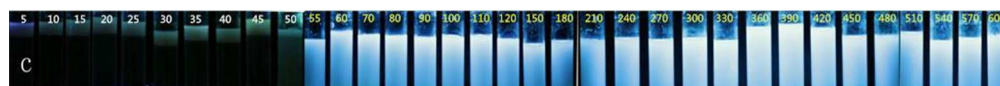


Fig.1 (c) Pictures of ongoing reacting fluorescent acrylate emulsion taken by camera varied with reaction time (From 5 to 600min)

271x21mm (96 x 96 DPI)



Fig.2 (a) Fluorescent acrylate emulsion and ordinary acrylate emulsion irradiated under UV light

163x128mm (96 x 96 DPI)

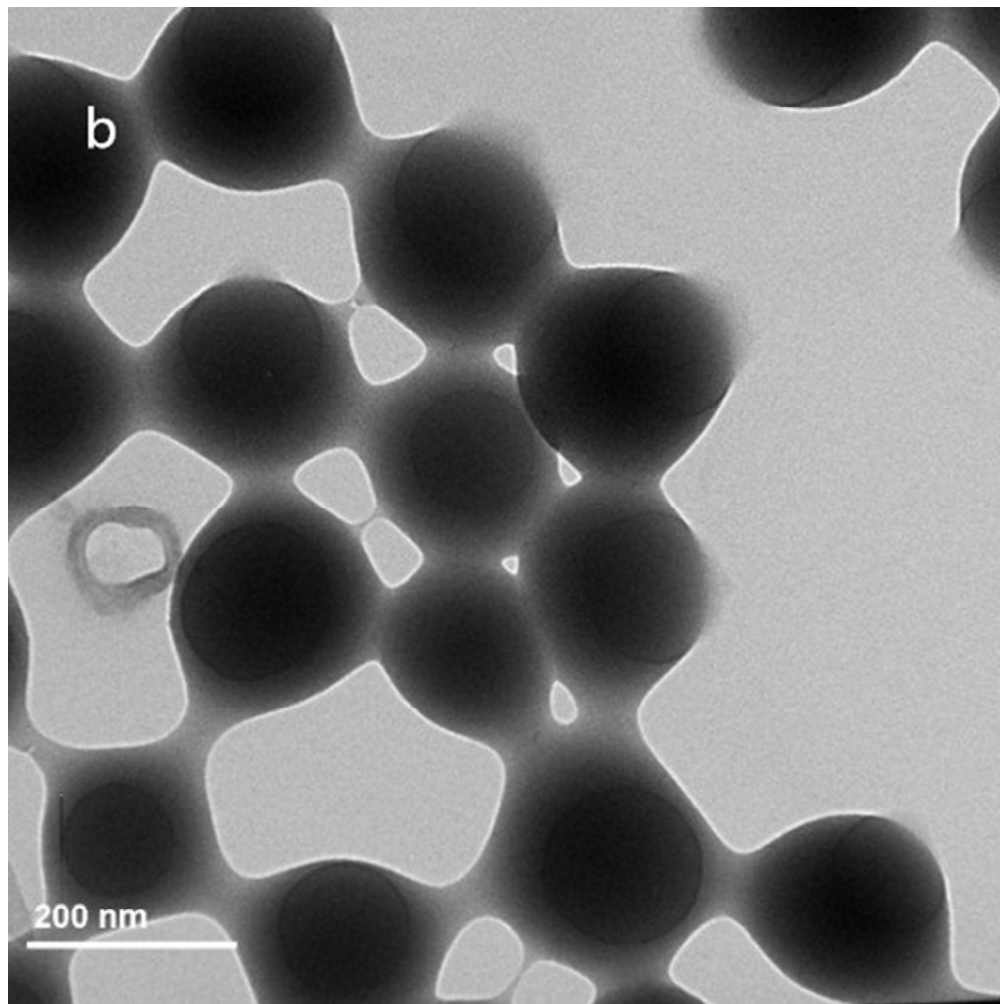


Fig.2 (b) Fluorescent acrylate emulsion observed from TEM measurement

134x134mm (96 x 96 DPI)

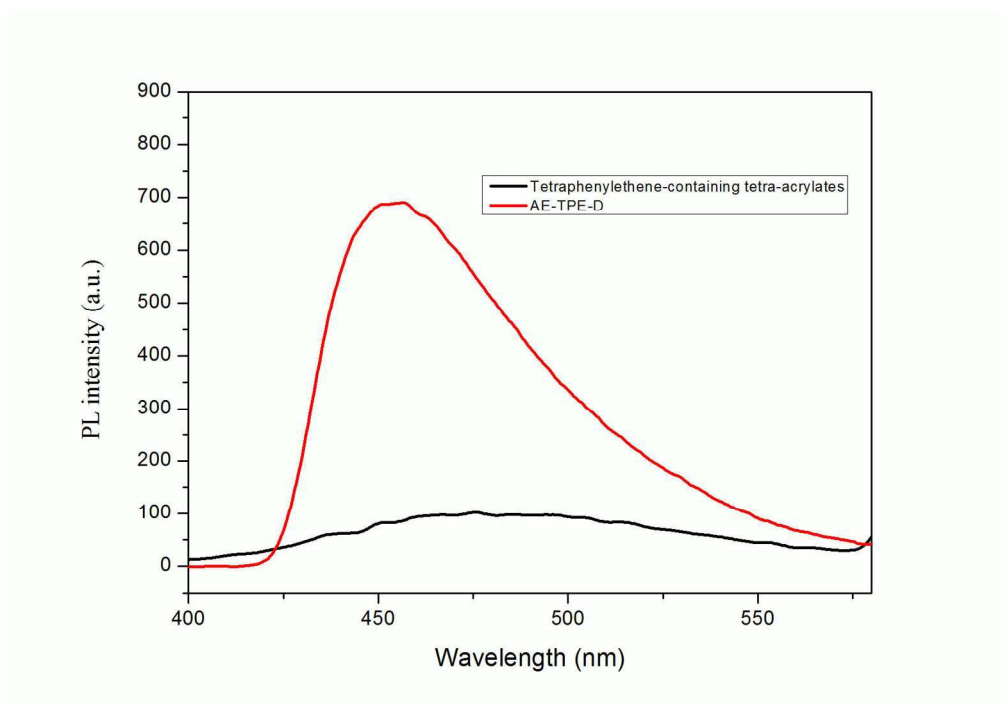


Fig.3 Fluorescence spectra of TPE-containing tetra-acrylate in THF-water (1:99) mixture and Fluorescent Acrylate emulsion (AE-TPE-D)

464x324mm (96 x 96 DPI)

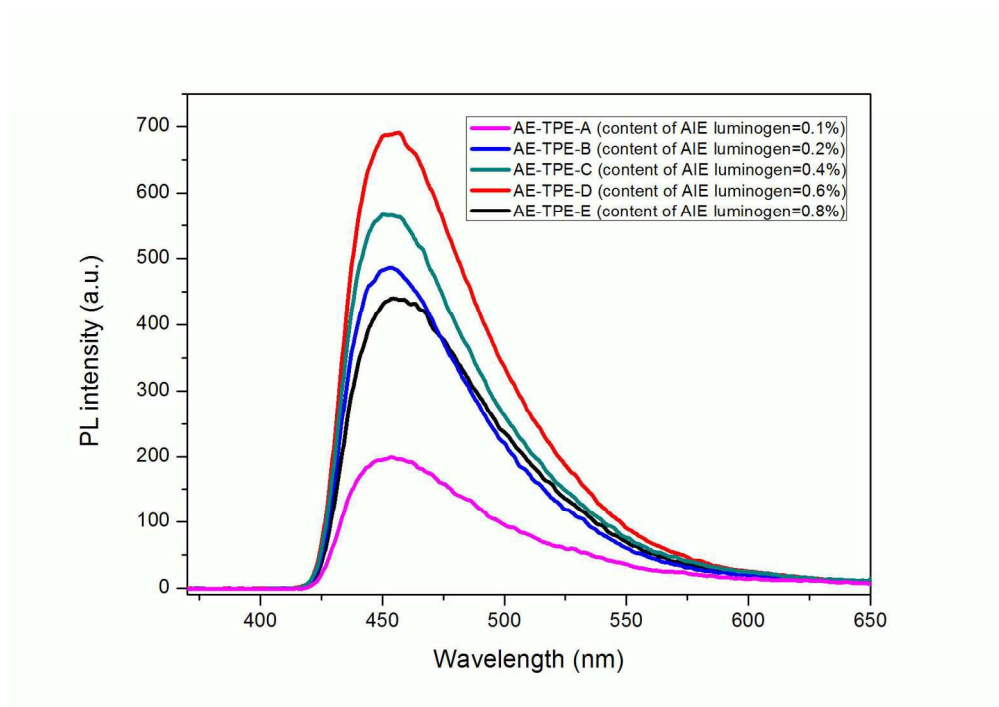


Fig.4 Fluorescence spectra of Fluorescent Acrylate emulsion varied with the content of TPE-containing tetra-acrylate

464x324mm (96 x 96 DPI)

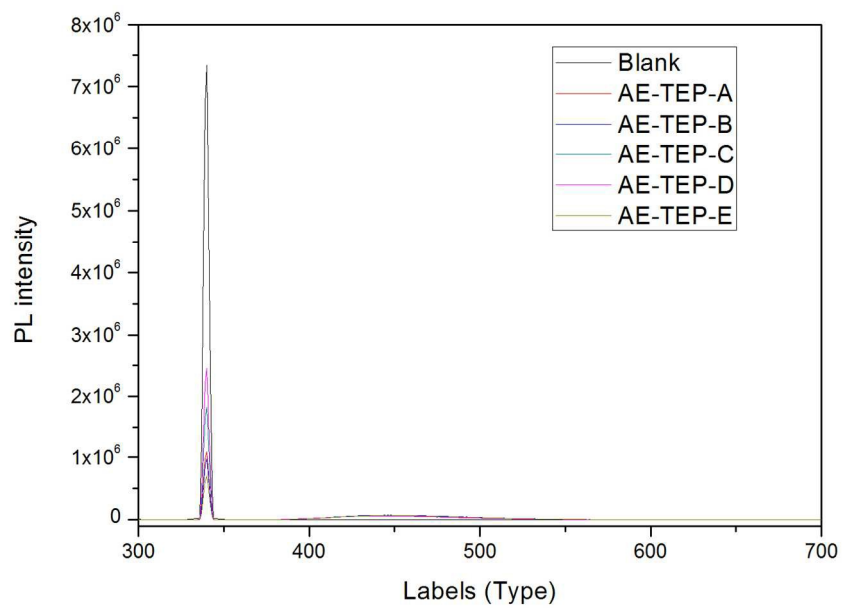


Fig.5 Fluorescence quantum yield(Φ_F) of fluorescent acrylate emulsions varied with the content of AIE luminogen

289x202mm (150 x 150 DPI)

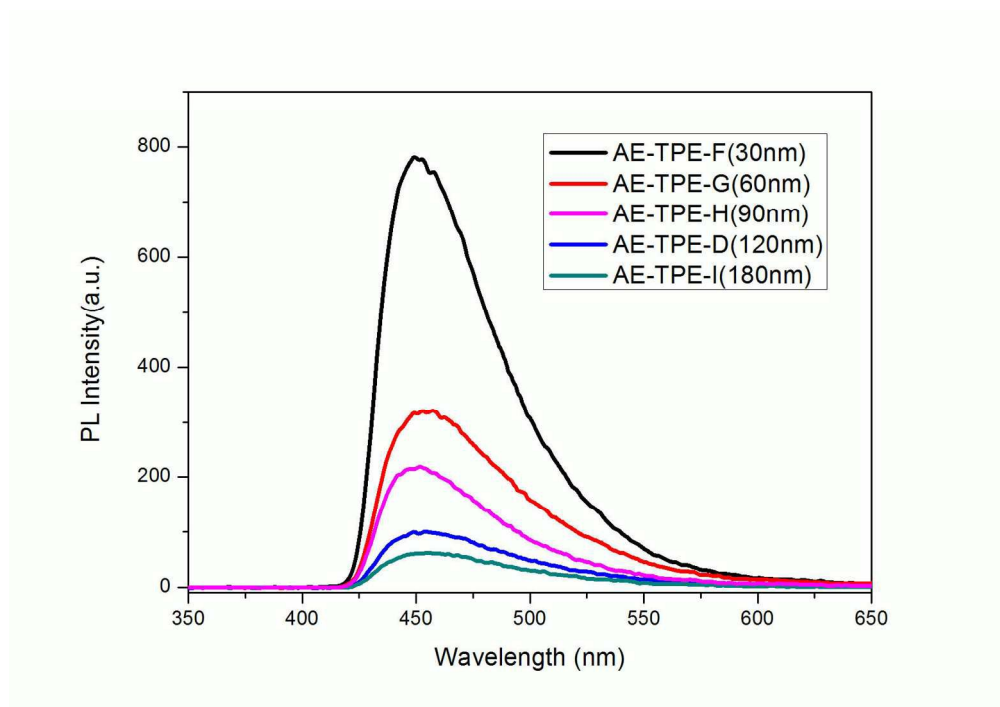


Fig.6 Fluorescence spectra of fluorescent acrylate emulsion varied with particle size

464x324mm (96 x 96 DPI)

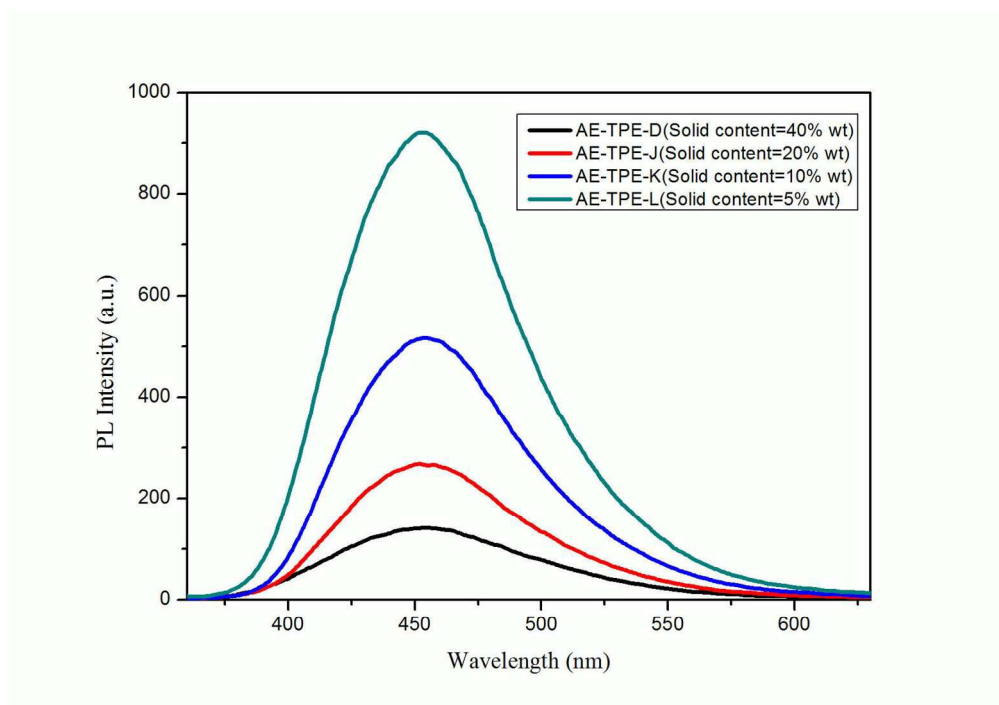


Fig.7 Fluorescence spectra of fluorescent acrylate emulsion(AE-TPE-D) varied with their concentration

464x328mm (96 x 96 DPI)

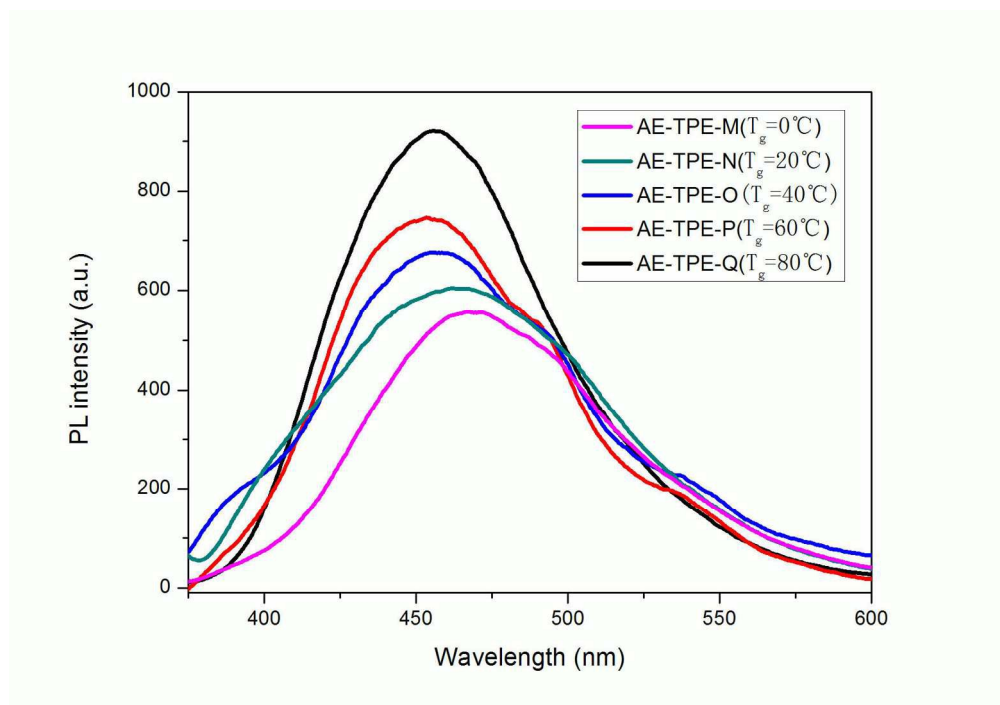


Fig.8(a) Fluorescence spectra of fluorescent acrylate emulsiones varied with their Tg values

464x324mm (96 x 96 DPI)

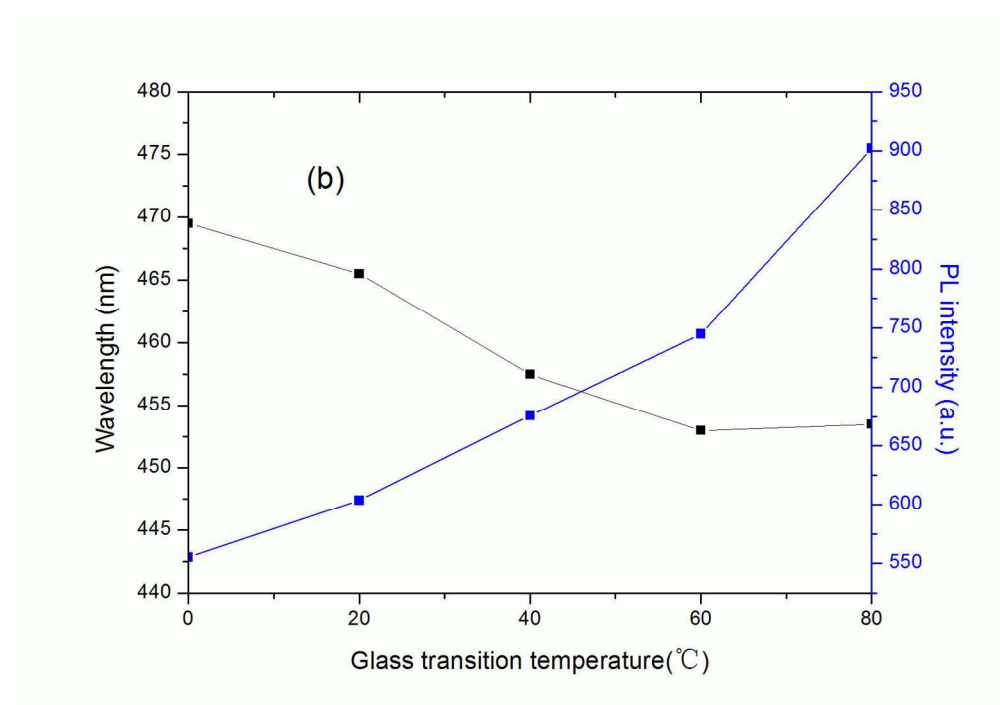


Fig.8 (b) Fluorescent wavelength & intensity of fluorescent acrylate emulsion varied with their T_g values

464x324mm (96 x 96 DPI)

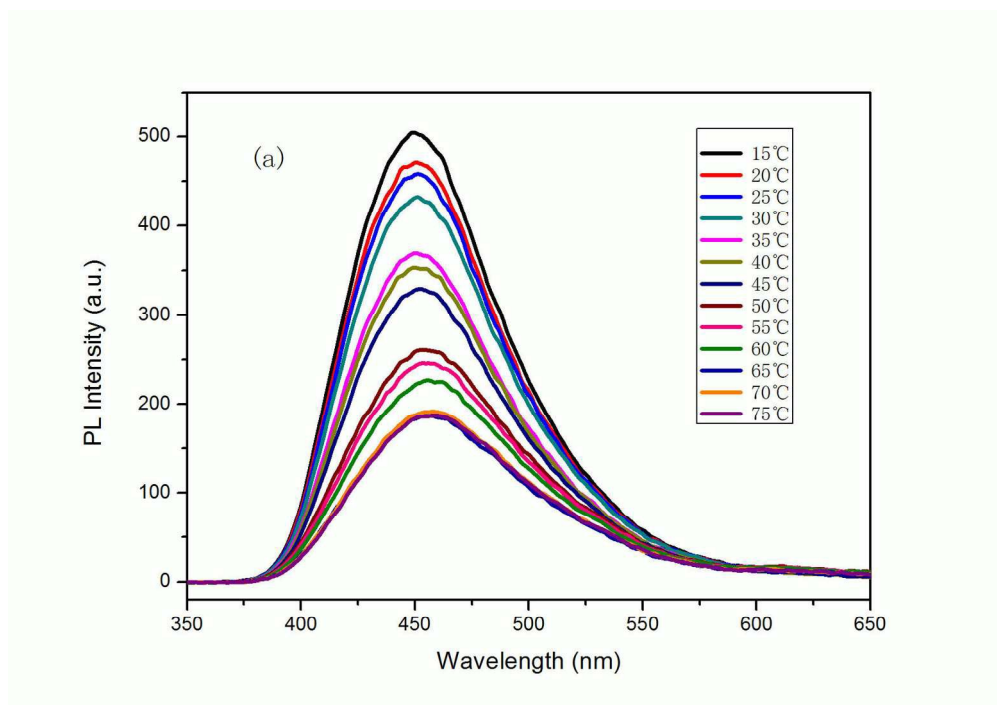


Fig.9(a) Fluorescence spectra of fluorescent acrylate emulsion (AE-TPE-P, T_g=40°C) varied with the testing temperature

464x328mm (96 x 96 DPI)

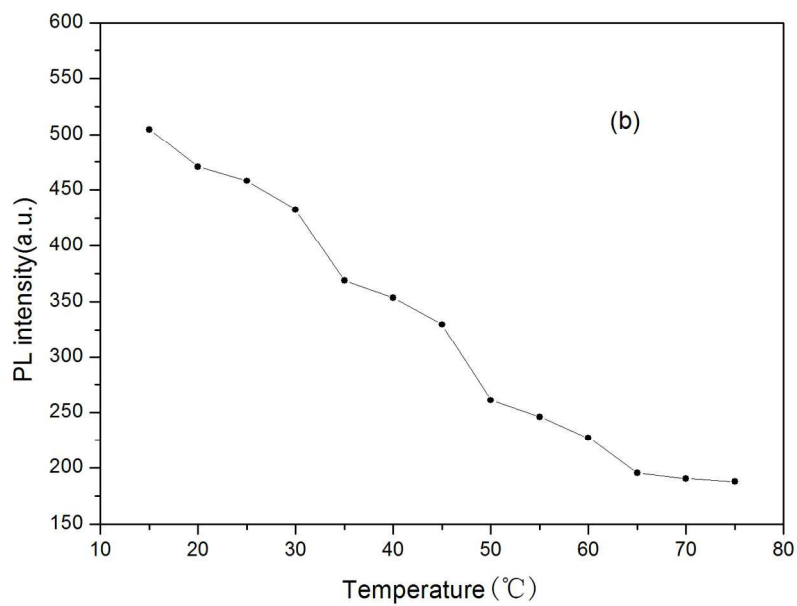


Fig.9 (b) fluorescent intensity of AE-TPE-P varied with the testing temperature

464x324mm (96 x 96 DPI)

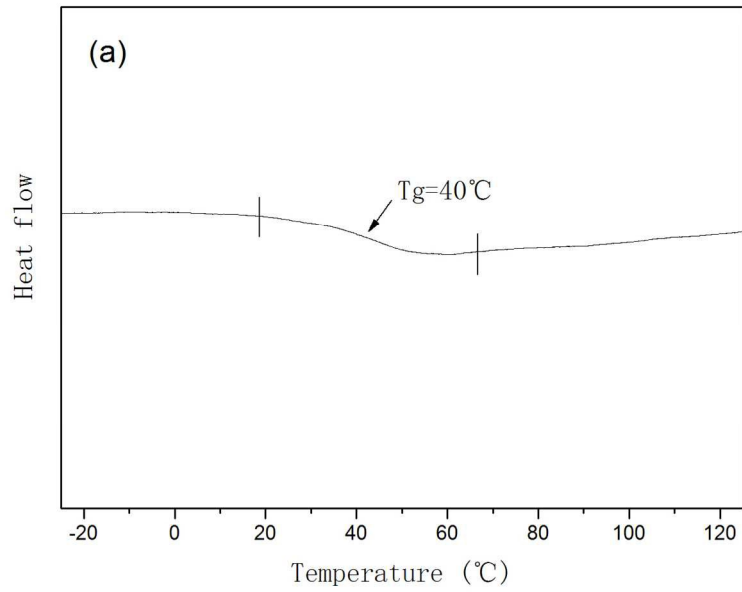


Fig.10 Study the properties of the dried AE-TPE-P powders by different testing methods (a) DSC thermograms

450x314mm (96 x 96 DPI)

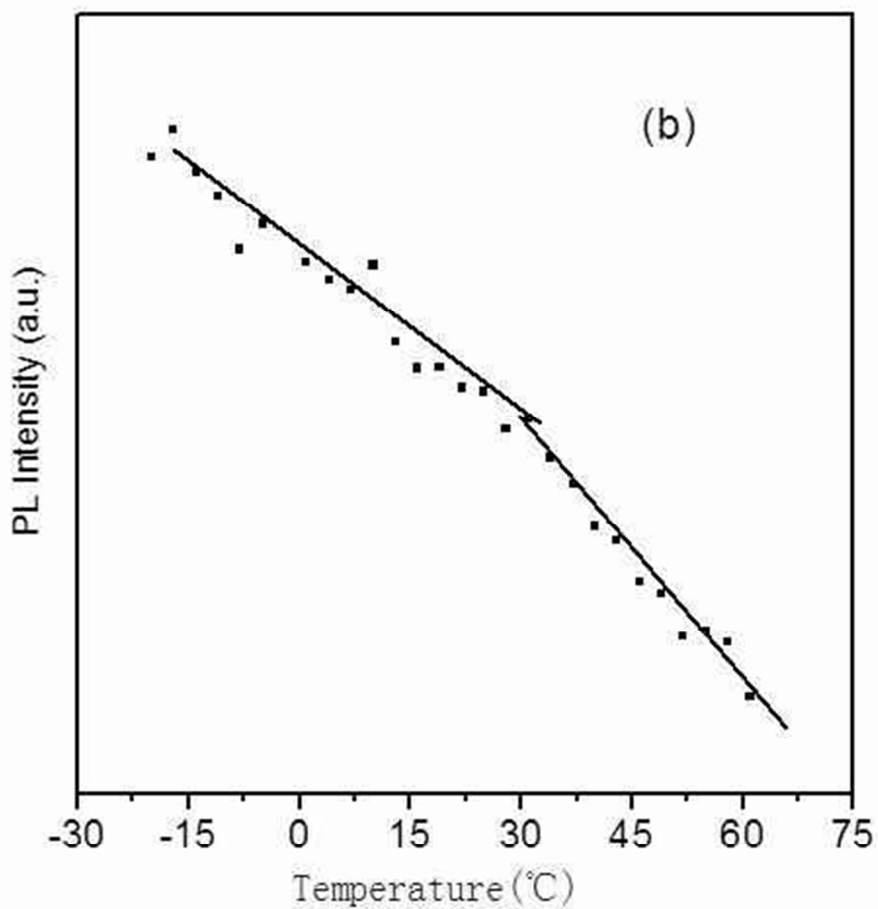
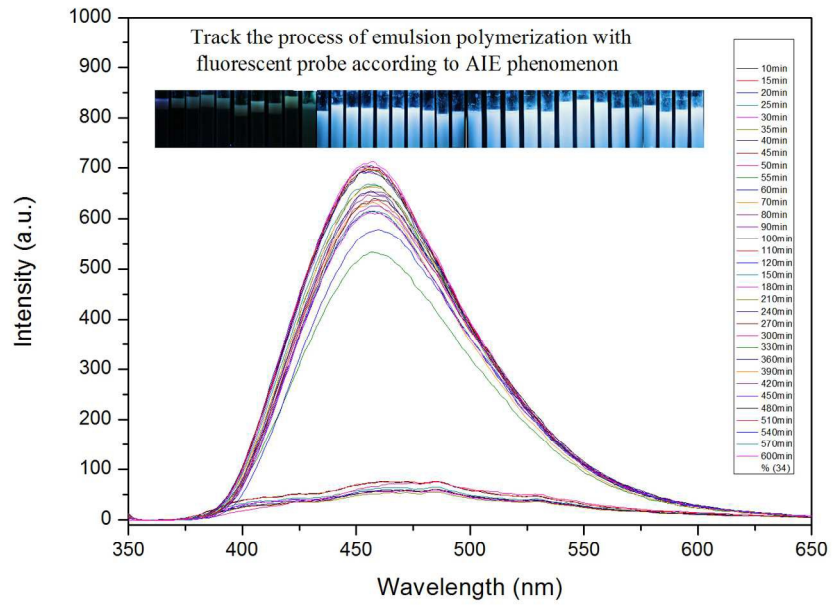


Fig.10 (b) PL intensities of dried AE-TPE-P varied with test temperature

135x129mm (96 x 96 DPI)



464x328mm (96 x 96 DPI)